Progress In Electromagnetics Research C, Vol. 47, 103–109, 2014

A Multi-Status Behavioral Model for the Elimination of Electrothermal Memory Effect in DPD System

Huadong Wang*, Hong Ma, and Jinfeng Chen

Abstract—In this paper, a behavioral model with multi-status is represented to describe electrothermal memory of power amplifiers. In the model, a multi-point linearity approximation method is introduced to estimated the model coefficients at random status. The parameters of the new model can be identified by traditional identification algorithms such as recursive least square (RLS) with the input and feedback data at predetermined status points captured by the digital predistortion (DPD) system. Compared with traditional models, the coefficients estimation speed for the new model at new status is very fast. The final experiment result proves that the multi-status model can efficiently ameliorate the performance deterioration caused by electrothermal memory in the the DPD system, and at the same time it still keeps very high DPD performance.

1. INTRODUCTION

The research on the behavioral model of power amplifiers (PAs) yields many helpful results due to the development of wireless communication technology in the last decade [1–5]. Many new nonlinear memory models, such as general memory polynomial (GMP) [3, 4, 6], are introduced to describe the output characteristic of power amplifier, and experiment results show that these models exhibit very good performance for the description the characteristic of the wide-band power amplifiers. However, in those works, only the stable characteristic of power amplifiers has been discussed, and the transient characteristic, which is often influenced by a new physical phenomenon called electrothermal memory [7], is ignored in analysis.

The electrothermal memory effect, also called long term memory effect, is used to describe the difference between the outputs of the PA at different status. It is well known that the DPD system needs to update model coefficients when the output power of the PA changes; otherwise the performance of the DPD system is worsened by the status change of the PA. In the traditional DPD systems, the electrothermal memory effect can be eliminated by the adaptive predistortion algorithms, and its influence on output signal is trivial since the response time of the DPD system is usually very short. Unfortunately, for the system with rapid power variation, the effect of status variation must be taken into consideration in the the DPD model since the response time of the DPD system can not be neglected compared with the normal signal period; otherwise the electrothermal memory effect will greatly worsen the performance of the DPD system because the DPD will often be a wrong work status.

Recently, several methods have been introduced to predict electrothermal memory of power amplifiers [8–10]. In [8], a multiple time-scale PA model, in which FET's gate-source overdrive voltage of power amplifier is selected as parameter of model coefficients, is represented. In [9], a dynamic model parameter estimation method is introduced, and input signal is also used as status parameter. In [9], an additional model is used to describe long term memory, and the temperature of the transistor is selected as the status parameter of the model. However, those models are only used to fit the output

Received 28 November 2013, Accepted 23 January 2014, Scheduled 7 February 2014
* Corresponding author: Huadong Wang (wanghuadong1977@hotmail.com).
The authors are with the Telecommunication Department, Huazhong University of Science and Technology, China.

characteristic of the power amplifier on the computer, and the actual performance of these models in the DPD system is not discussed.

In this paper, a model with multi-status is introduced to describe the electrothermal memory of power amplifiers. To improve the speed and performance of the model identification, a multi-point linear approximation method is used for the estimation of the model coefficient. Finally, the new model has been applied to the DPD system in our transmitter to predict the electrothermal memory of power amplifiers, and experiment verifies that the new model can greatly improve transient performance of the DPD system compared with the traditional model.

2. DESCRIPTION OF DIGITAL PREDISTORTION AND THE MULTI-STATUE BEHAVIORAL MODEL

The architecture of the DPD is shown in Fig. 1, which is based on indirect learning architecture given in the literature [11]. The complex baseband samples at the input and output of the PA are recorded and used for the identification of the nonlinear model $F(s)$, in which s is status variant of the model. After $F(s)$ is identified, its coefficients can be directly assigned to the predistortion (PD) model. And the accurate PD coefficients can be obtained after several DPD iterations.

Different from the research on the traditional behavioral models, in which a optimal model is searched for the best stable performance of the DPD system, $F(s)$ in Fig. 1 is used to eliminate electrothermal memory effect from the output of the PA, which means that $F(s)$ should be able to describe the variation of the model coefficients when the status of the PA changes. It implies that the model coefficients can be regraded as the function of s, and the expression of $F(s)$ can be written as (1), where y is the baseband output signal, x the baseband input signal, and θ the model coefficient.

$$y = F(x, \theta(s)) \tag{1}$$

In most cases, the output power of the PA is used as status variant because it is the best figure of merit to describe the status of power amplifiers. The output power can be calculated by (2).

$$s(n) = \frac{1}{N_a} \sum_{k=n-N_a+1}^{n} |y(|k|)|^2 \tag{2}$$

in which N_a is the sample number for calculating average power.

As discussed above, the nonlinear expression is used to describe stable characteristic of the PA. Because we pay more attention to transient characteristic of the DPD system, the complexity of the model is not important during our analysis, and the memory polynomial model, which is widely used in DPD research due to its simplicity as shown in (3), is used in our research. A block diagram of the final model is shown in Fig. 2.

$$y_{\mathrm{MP}}(n) = \sum_{m=0}^{M_c} \sum_{k=1}^{N_c} \theta(s)_{m,k} x(n-m)|x(n-m)|^{k-1} \tag{3}$$

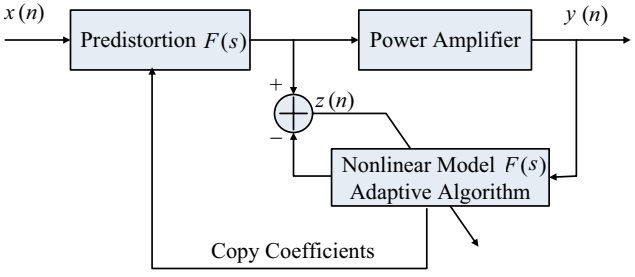

Figure 1. The architecture of the DPD system based on indirect learning architecture.

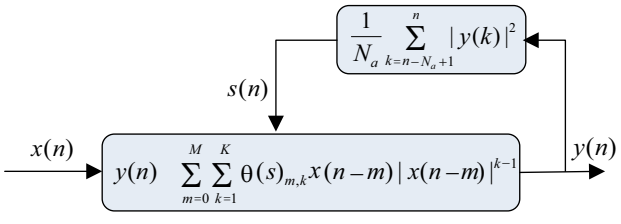

Figure 2. The block diagram of the proposed model with state variant.

3. IDENTIFICATION OF NONLINEAR MODEL

For the behavioral models based on the polynomial structure, the output $y_{\mathrm{MP}}(n)$ is proportional to the model coefficients $\theta(s)_{m,k}$, and the output signals at status s_1 and s_2 can be written as following.

$$y_{\mathrm{MP}}(n)_{s_1} = \sum_{m=0}^{M_c}\sum_{k=1}^{N_c}\theta(s_1)_{m,k}x(n-m)|x(n-m)|^{k-1} \tag{4}$$

$$y_{\mathrm{MP}}(n)_{s_2} = \sum_{m=0}^{M_c}\sum_{k=1}^{N_c}\theta(s_2)_{m,k}x(n-m)|x(n-m)|^{k-1} \tag{5}$$

For the random status s_r in the range of (s_1, s_2), s_r can be represented as as_1+bs_2, where $a+b=1$. If the linear approximation method is used to estimate the value of $y_{\mathrm{MP}}(n)$ at status s_r as shown in Fig. 3, we can obtain the following expression.

$$y_{\mathrm{MP}}(n)_{s_r} = ay(n)_{s_1} + by(n)_{s_2} \tag{6}$$

Applying Equations (4) and (5) in (6), the output at status s_r can be written as following.

$$\begin{aligned} y_{\mathrm{MP}}(n)_{s_r} &= \sum_{m=0}^{M_c}\sum_{k=1}^{N_c}(a\theta(s_1)_{m,k} + b\theta(s_2)_{m,k})x(n-m)|x(n-m)|^{k-1} \\ &= \sum_{m=0}^{M_c}\sum_{k=1}^{N_c}\theta(s_r)_{m,k}x(n-m)|x(n-m)|^{k-1} \end{aligned} \tag{7}$$

where

$$\theta(s_r)_{m,k} = a\theta(s_1)_{m,k} + b\theta(s_2)_{m,k} \tag{8}$$

Applying $s_r = as_1 + bs_2$ into Equation (8), the estimation equation of the model coefficient $\theta(s)$ with linear approximation can be deduced. To improve the fitting precision, a multi-points linear approximation method is used in our system, and its expression is given as following.

$$\theta(s) = \begin{cases} \theta(s_i) + \dfrac{\theta(s_j)-\theta(s_i)}{s_j - s_i}(s-s_i) & s_i < s < s_j \\ \theta(s_1) + \dfrac{\theta(s_2)-\theta(s_1)}{s_2 - s_1}(s-s_1) & s < s_1 \\ \theta(s_k) + \dfrac{\theta(s_k)-\theta(s_{k-1})}{s_k - s_{k-1}}(s-s_k) & s > s_k \end{cases} \tag{9}$$

where s_1, s_2, ..., s_k are predetermined status points which are used as identified the multi-stage straight line used in multi-point linear approximation method as shown in the Fig. 3. $\theta(s_1)$, $\theta(s_2)$, ..., $\theta(s_k)$ are the model coefficients at different predetermined status points.

It is clear that $\theta(s_1)$, $\theta(s_2)$, ..., $\theta(s_k)$ in (9) must be identified before the model is used to estimate the model coefficients at other status. Actually, $\theta(s_i)$ can be calculated by solving Equation (10) with least means squares (LMS) method or RLS method when the input and feedback data at status s_i are captured. In our DPD system, the RLS method is used in for the solution of matrix Equation (10).

$$Y = X * A(s_i) \quad i \in 1, 2, 3, \ldots, k \tag{10}$$

where Y is the output vector, X the input matrix, and $A(s_i)$ the coefficient vector with state s_i, whose definitions are given as following, where M_a is the number of model coefficient.

$$X = [x(n), \ldots, x(1)]^T \tag{11}$$

$$Y = [Y_n, \ldots, Y_1]^T \tag{12}$$

$$Y_n = [y(n)_{s_i}, \ldots, y(n)_{s_i}|y(n)_{s_i}|, \ldots, y(n-m)_{s_i}|y(n-m)_{s_i}|, \ldots]^T \tag{13}$$

$$A(s) = [\theta_1(s_i), \ldots, \theta_{M_a}(s_i)]^T \tag{14}$$

Obviously, the computation complexity of $\theta(s_i)$ at random status with Equation (9) is far less than that of the traditional model identification method by solving Equation (10), which illustrates that the new model can greatly reduce the effect of electrothermal memory effect to the DPD system.

4. DESCRIPTION OF THE EXPERIMENT SYSTEM

The nonlinear order N and memory depth M of the MP model in our system are 7 and 3, respectively. And the number of predetermined status points can be decided by the rule of the thumb. The PD module is implemented in the field programmable gate array (FPGA) device, and the identification algorithm of the DPD model is executed in the embedded processor MicroBlaze in the FPGA. A power statistics module is used in the feedback path to monitor the variation of the output power periodic.

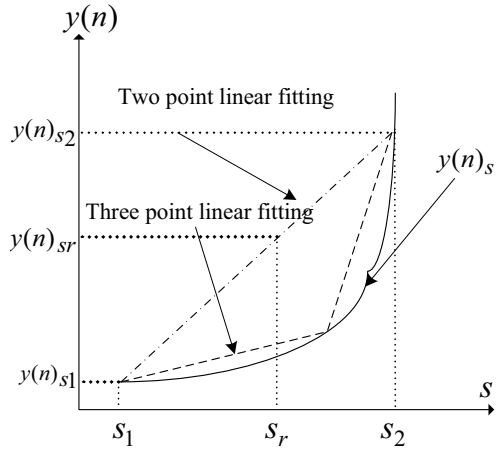

Figure 3. The plot of the output signal $y(n)$ vs status variants s.

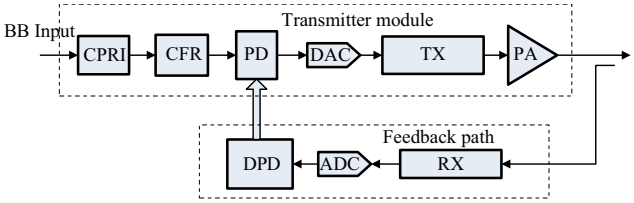

Figure 4. Block diagram of the RRU system.

The structure of the remote radio unit (RRU) is shown in Fig. 4, which consists of the digital intermediate frequency module with FPGA and digital to analog converter (DAC), transmitter unit with the frequency up-conversion units and variable gain amplifier (VGA) units, 10-W Doherty power amplifier designed using MRF8P26080 LDMOS transistors, and feedback unit with sample rate 184.32 MHz which is used to capture the signal from the output of the PA and to test the performance of our model.

The setup shown in Fig. 5 is considered for model performance evaluation purposes. The time division long term evolution (TD-LTE) baseband signal generated from the building baseband unit (BBU) is transmitted to RRU for performance test and the output spectrum of power amplifier is captured by the vector signal analyzer. The computer is connected with RRU through local area network (LAN) and RS232 for data transmission.

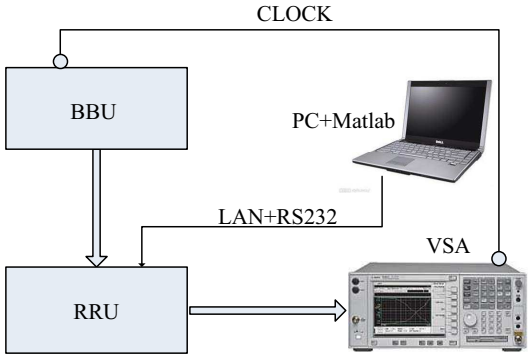

Figure 5. Functional diagram of the laboratory setup used for the the multi-status behavioral model evaluation.

5. PERFORMANCE ANALYSIS OF INTERPOLATION

To evaluate the performance of the model with multi-status, the normalized mean square errors (NMSEs), whose definition is given in (10), of the models with different predetermined status points are compared in Fig. 2, where $y_m(n)$ represents the model output.

In Fig. 6, $S1$, $S2$ and $S3$ represent three linear approximation results with different predetermined status points, and $E1$ and $E2$ represent the cases that the model coefficients at 33 dBm and 39 dBm are directly used to other status points respectively. Finally, the model whose coefficient at all status points are identified by traditional methods is given as $T1$ for the comparison.

It is clear that $E1$ and $E2$ describe the transient performance of the traditional memory polynomial model, and min($E1$, $E2$) describes the transient performance of model in [8] with two status points. If we define $\theta(s_i)$ in (5) to be θ_0 and $(\theta(s_j) - \theta(s_i))/(s_j - s_i)$ to be θ_1, our model is equal to the model given by [9], which means that $S1$ can describe the transient performance of that model. Compared with $E1$ and $E2$, both min($E1$, $E2$) and $S1$ have higher model precision, which proves their abilities to describe the transient characteristic of power amplifiers. However, the performance enhancement of those models is limited since the model performances at status points far from predetermined status points have no obvious improvement.

This problem can be solved by the increase of the predetermined status points, and the result in the figure illustrates that the model with 4 predetermined status points has far less NMSE than the model with 2 predetermined status points since $S3$ is far better than $S1$, which also verifies that the new model can obtain higher precision than the models in [8, 9]. The analysis result also shows that 4 predetermined status points are enough for our system, which are predetermined as 33 dBm, 35 dBm, 37 dBm, and 39 dBm, respectively.

$$\text{NMSE (dB)} = 10 * \log_{10} \frac{\sum_{n=1}^{N} |y_m(n) - y(n)|^2}{\sum_{n=1}^{N} |y(n)|^2} \tag{15}$$

It should be mentioned that the main fitting error in Fig. 6 should be owned to normalized process of feedback signal before model identification since the output power of our transmitter is controlled by VGA in radio frequency (RF) module. For the transmitter with fixed gain in the RF module, the fitting error will be far less than our transmitter, and our model will exhibit better performance than that shown in Fig. 6.

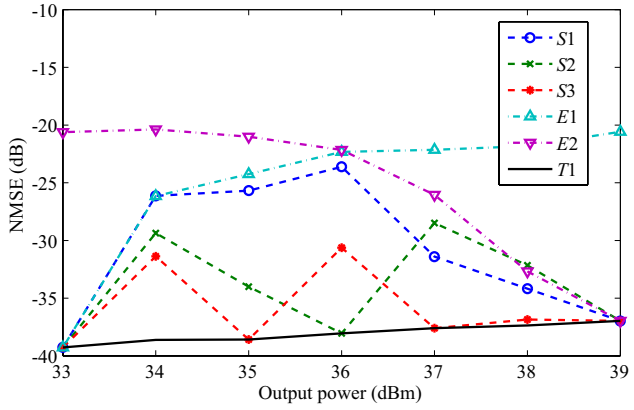

Figure 6. The comparison of performances of the multi-status models based on memory polynomial with different interpolation coefficients.

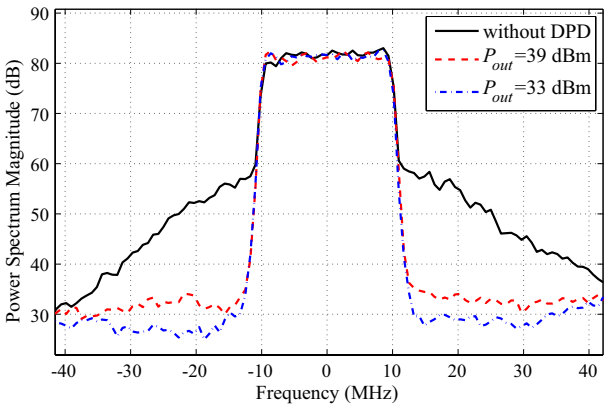

Figure 7. The output spectrum of the power amplifier before and after DPD.

6. MEASUREMENT RESULT

The stable performances of the power amplifier before and after DPD are shown in Fig. 7. The adjacent channel power ratio (ACPR) of the power amplifier at 33 dBm output after DPD is less than −57 dB, more than 27 dB better than that before DPD, and the improvement of the ACPR at 39 dBm output is about 22 dB, 5 dB worse than the improvement at 33 dBm. This result shows that the DPD with the MP model exhibits different performances at different outputs, which implies that the DPD system should respond to the variance of the output rapidly for the sake of the total performance enhancement.

To evaluate the transient performance of the new model in the DPD application, a time-varying TD-LTE signal shown in Fig. 8 is used in system test. To eliminate the effect of the adaptive DPD algorithm to the transient characteristic of the model, the update time of the PD module is predefined to be the middle of each signal period. By this method, the transient performance of the traditional MP model can be compared with that of the new model in the time domain.

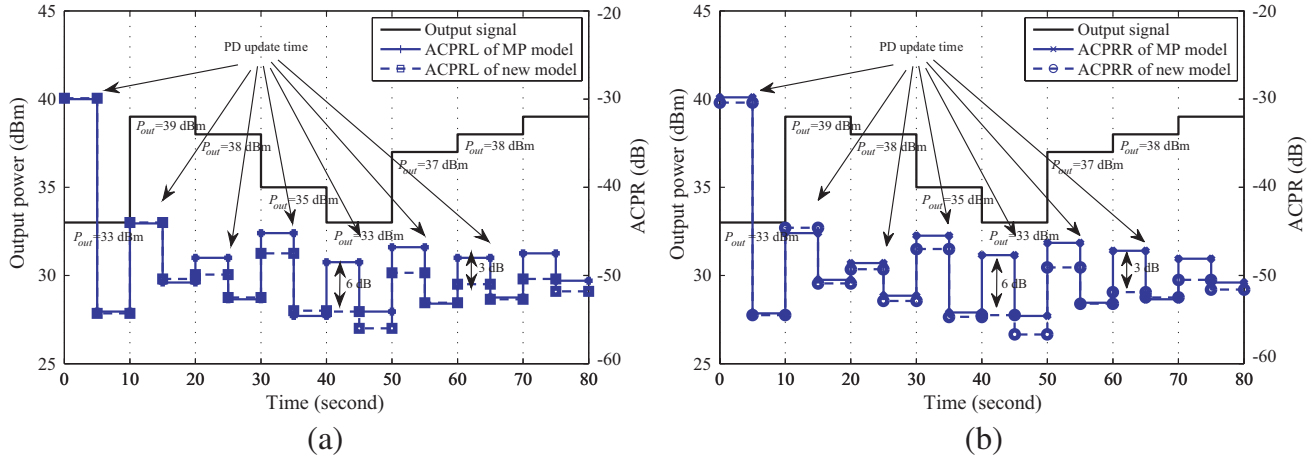

Figure 8. The comparison of ACPRs of output signals of traditional DPD model and DPD model with multi-status with regular power variation TD-LTE signal, where ACPRL represents the left adjacent channel power ratios and ACPRR represents the right adjacent channel power ratios. ((a) ACPRL of output signals; (b) ACPRR of output signal.).

Fig. 8 shows that after initial model identification, the new model exhibits better transient performance than the traditional MP model. When output power varies, the new model also changes rapidly, and the ACPR of new DPD model is far less than that of the traditional DPD model. The results at the time instants $t = 40$ s and $t = 70$ s show that the new model can accurately store and predict power amplifier's characteristic at predetermined status points, which proves that electrothermal memory can efficiently eliminated by the new model at these status points. Furthermore, the effect of electrothermal memory at other status can also be weakened by the new model, which illustrates the new model's ability to improve the transient performance of the DPD system.

Comparing the result at the time instants $t = 20$ s with that at $t = 60$ s, we find that the new model can update model parameter instantly with the variation of the predetermined status points. The ACPR at $t = 20$ s is 2 dB worse than that at $t = 60$ s, which illustrates that the model with 4 predetermined status points has higher model parameter estimation precision than the model with 2 predetermined status points since at the former case only two predetermined status points (33 dBm and 39 dBm) are identified, and at latter case, all four predetermined status points are identified. This result is consistent with the conclusion given by Fig. 6, and a suitable number predetermined status points must be determined before model identification to obtain high transient performance for the DPD application.

7. CONCLUSION

In this paper, a multi-status behavioral model is proposed to predict electrothermal memory effect of power amplifiers. By introducing status variant and linear interpolation, the transient performance of power amplifier can be predicted rapidly and accurately. The experiment shows that our model exhibits better transient performance than known models in the DPD application, which verifies the new model's ability to eliminate the electrothermal memory of the PA in DPD system.

REFERENCES

1. Pedro, J. C. and S. A. Maas, "A comparative overview of microwave of microwave and wireless power-amplifier behavioral modeling approaches," *IEEE Trans. on Microw. Theory and Tech.*, Vol. 53, No. 4, 1150–1163, 2005.
2. Isaksson, M., D. Wisell, and D. Ronnow, "A comparative analysis of behavioral models for RF power amplifiers," *IEEE Trans. on Microw. Theory and Tech.*, Vol. 54, No. 1, 348–358, 2006.
3. Yuan, X. H. and Q. Feng, "Behavioral modeling of RF power amplifiers with memory effects using orthonormal hermite polynomial basis neural network," *Progress In Electromagnetics Research C*, Vol. 34, 239–251, 2013.
4. Du, T., C. Yu, J. Gao, Y. Liu, S. Li, and Y. Wu, "A new accurate volterra-based model for behavioral modeling and digital predistortion of RF power amplifiers," *Progress In Electromagnetics Research C*, Vol. 29, 205–218, 2012.
5. Hammi, O., M. Younes, A. Kwan, M. Smith, and F. M. Ghannouchi, "Performance-driven dimension estimation of memory polynomial behavioral models for wireless transmitters and power amplifiers," *Progress In Electromagnetics Research C*, Vol. 12, 173–189, 2010.
6. Morgan, D., Z. Ma, and J. Kim, "A generalized memory polynomial model for digital predistortion of RF power amplifiers," *IEEE Trans. on Signal Process.*, Vol. 54, No. 10, 3852–3860, 2006.
7. P. Robin, D. E. Root, J. Verspecht, Y. Ko, and J.Teyssoer, "New trends for the nonlinear measurement and modeling of high-power RF transistors and amplifiers with memory effects," *IEEE Trans. on Microw. Theory and Tech.*, Vol. 60, No. 10, 3852–3860, 2012.
8. Pedro, J. C, P. M. Cabral, T. R. Cunha, and P. Lavrador, "A multiple time-scale power amplifier behavioral model for linearity and efficiency calculations," *IEEE Trans. on Microw. Theory and Tech.*, Vol. 61, No. 1, 606–615, 2013.
9. Tehrani, A. S., T. Eriksson, and C. Fager, "Modeling of long term memory effects in RF power amplifiers with dynamic parameters," *IEEE MTT-S Int. Microwave Symp. Dig.*, 1–3, Montreal, Canada, June 2012.
10. Cadenas, C. C., J. Tosina, and M. Madero, "Study of a power amplifier behavioral model with nonlinear thermal effects," *Proceedings of the 40th European Microwave Conference*, 1138–1141, Paris, France, September 2010.
11. Ding, L, G. T. Zhou, D. R. Morgan, Z. Ma, and J. S. Kenney, "A robust digital baseband predistorter constructed using memory polynomial," *IEEE Trans. on Commun.*, Vol. 52, No. 1, 159–165, 2004.